Supplementary material for "Estimation of ice ablation on a debris-covered glacier from vertical debris-temperature profiles"

Sourav Laha[1], Alex Winter-Billington[2], Argha Banerjee[1], R. Shankar[3], H.C Nainwal[4], Michele Koppes[2]

[1]Earth and Climate Science, Indian Institute of Science Education and Research, Pune, India

[2]Department of Geography, University of British Columbia, Vancouver, Canada

[3]The Institute of Mathematical Sciences, Chennai, India

[4]H.N.B Garhwal University, Uttarakhand, India

Correspondence: Sourav Laha <sourav.laha@students.iiserpune.ac.in>

S1 Supplementary text

S1.1 Monte Carlo procedure in Bayesian inversion technique

The steps involved in the stochastic minimisation procedure following a Monte Carlo procedure are as follows.

- Simulation started with randomly chosen model parameters (κ, s) for the debris layer within the mentioned range.
- Random corrections $\kappa + \epsilon\Delta\kappa$ and $s + \epsilon\Delta s$ were proposed for the model parameters (κ, s), and temperature profiles were simulated with the new set of parameters. Here, ϵ was a uniform random number in the range -1 to 1, and $\Delta\kappa$ and Δs were fixed step sizes.
- The proposed parameters were then accepted with metropolis probability (Gelman and others, 2013) of $\mathrm{Max}[1, e^{-\Delta\delta^2}]$, where $\Delta\delta^2$ is the difference between the δ^2 computed for the initial and the proposed models. Whenever the proposed set of parameters was accepted, the initial set of parameter values (κ, s) were replaced by corresponding proposed values.

This procedure was repeated to perform a random walk in the parameter space for up to 5000 iterations. Efficient sampling of the parameter space requires an acceptance rate approximately between 20–50% for the Monte Carlo approach (Gelman and others, 2013).

To achieve a reasonable acceptance rate, the step sizes $\Delta\kappa$ and Δs were tuned. First, we ran the MC for 5000 iterations for 9 pairs of ($\Delta\kappa$,Δs), with $\Delta\kappa$ (Δs) being 0.05, 0.025, and 0.0125 times the allowed range of κ (s) values. The mean acceptance rate over the last 2000 iterations in each of these runs were used to locate the ($\Delta\kappa$,Δs) pair value that gave an acceptance rate closest to 30%. Then, we zoomed around the neighborhood of the selected pair that was within a region ±30% of the selected values (supplementary Fig. S4), and 9 pairs of ($\Delta\kappa$,Δs) values were chosen to repeat the whole procedure. The pair that gave an acceptance rate closest to 30% among the 18 trial pairs of ($\Delta\kappa$,Δs) was chosen (supplementary Fig. S4). This procedure was performed separately for each of the records.

With the chosen step sizes ($\Delta\kappa$,Δs), we ran the Monte Carlo for 10000 iterations. To check the convergence of the model parameters, we ran five independent Monte Carlo simulations, each time with a different random initial model and with a different sequence of pseudo-random numbers. We checked the auto-correlations of the time series and inspected the distribution of sampled parameters to ensure efficient sampling. Finally, we used the set of all accepted states from the last 5000 iterations of each of these five independent runs for our final calculations. Out of all the selected states, the maximum-likelihood state, i.e., the model with a minimum value of δ^2, was used to compute the best-fit temperature profile and thermal diffusivities. For each of the temperature records analysed, the ensemble of accepted states was utilised for computing the corresponding uncertainties of the best-fit parameters.

S2 Supplementary figures

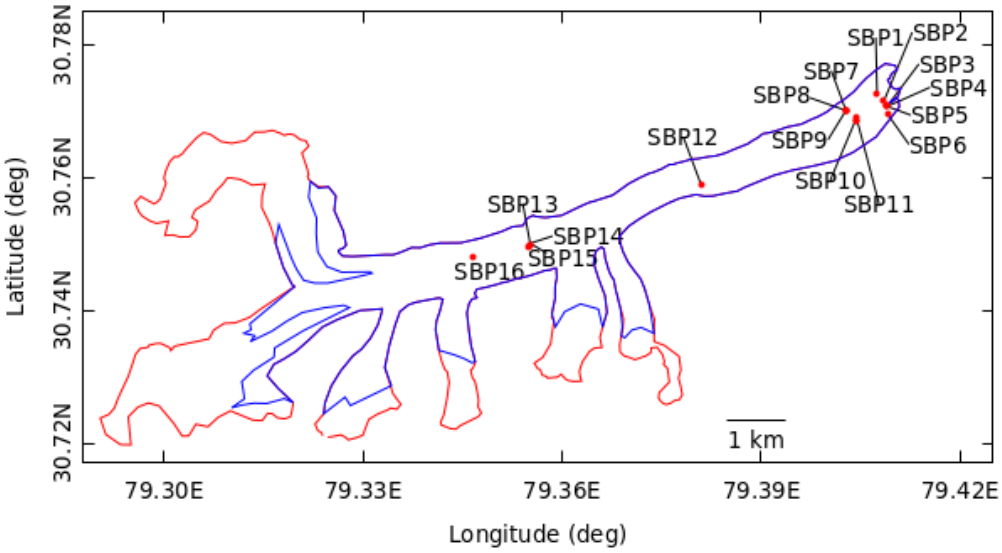

Fig. S1: Location of the 16 pits on Satopanth Glacier (Table 1, in the main text) are shown by solid red circles, labelled with the corresponding pit name. The solid red line is the glacier boundary, and the blue line is the extent of debris-covered on the glacier.

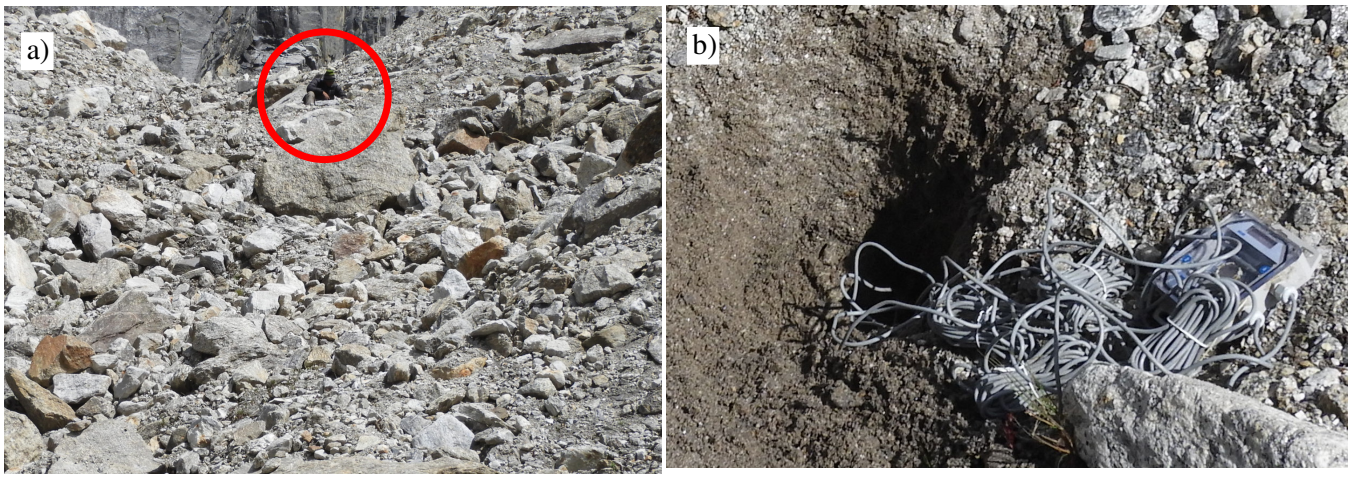

Fig. S2: a) Surrounding area of an example pit (SBP5). The red circle shows a person sitting near the pit. b) Pit SBP5 dug on Satopanth Glacier for temperature measurements. The temperature sensors are inserted on the pit wall and are connected to the data logger on the glacier surface.

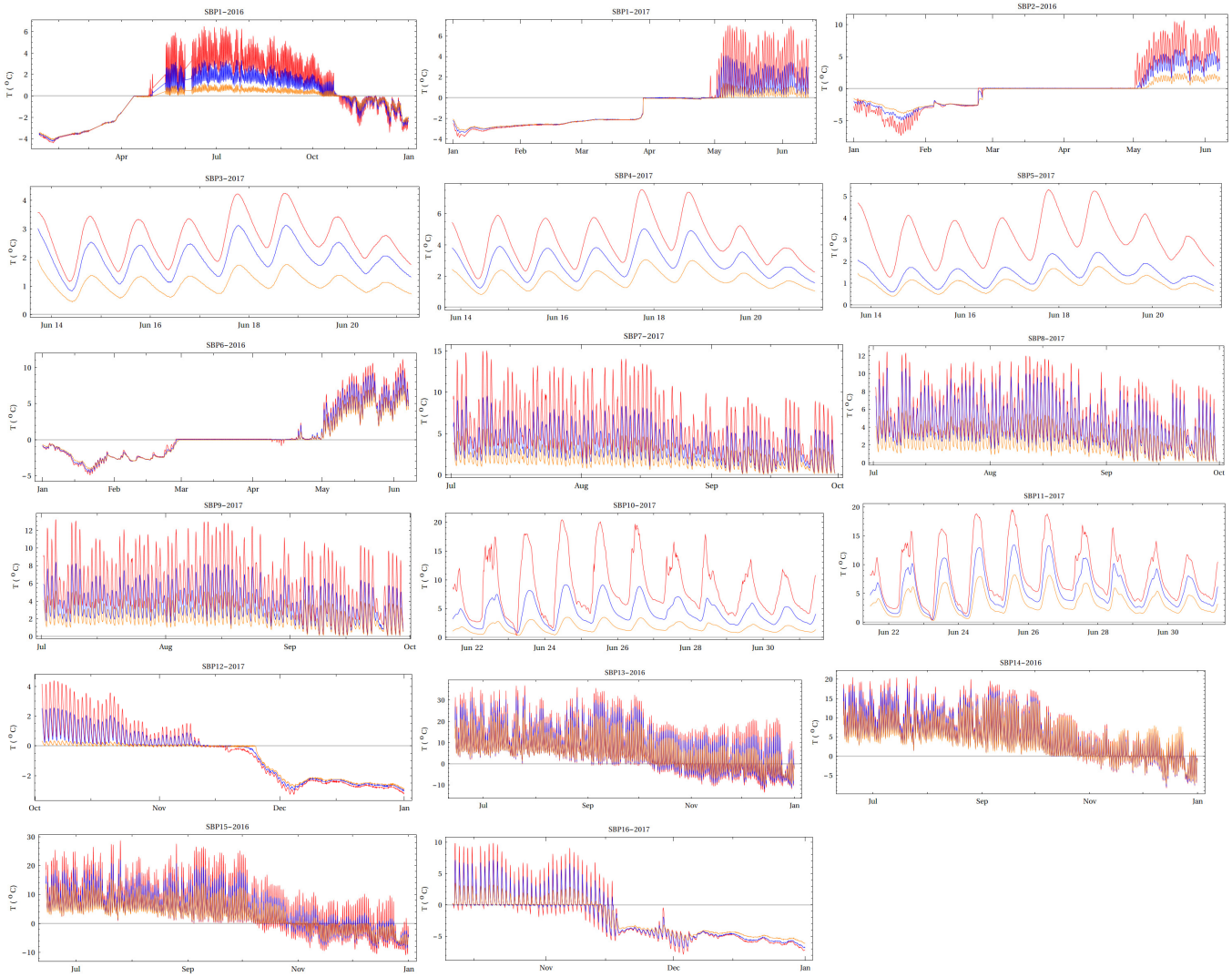

Fig. S3: Temperature time series recorded at three of the bottom-most sensors (Table 1 in the main text) are plotted for different pits. The temperature at vertical distances $z = -dz_1$, $z = 0$, and $z = dz_2$ (Fig 3 in the main text) are coloured by red, blue, and yellow, respectively.

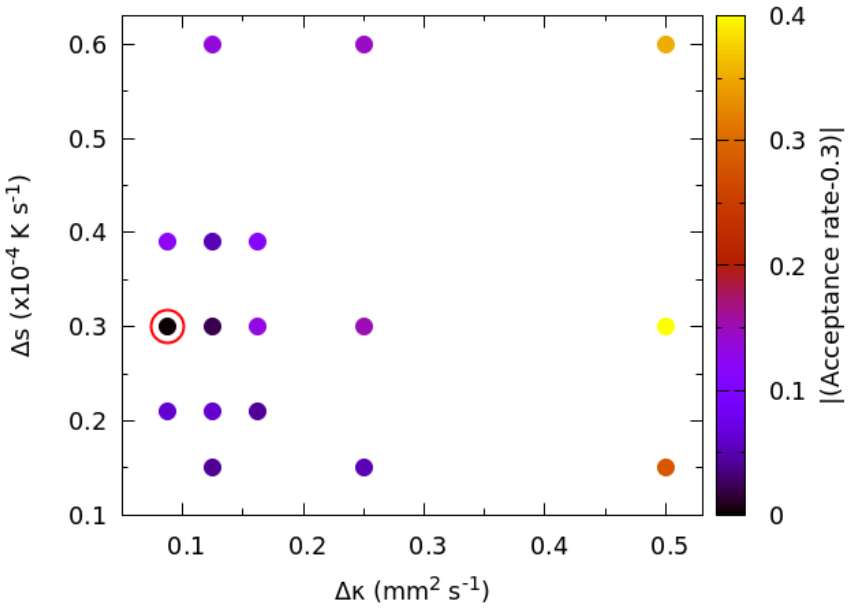

Fig. S4: An example of the grid search procedure in the Bayesian method to find the pair of step sizes ($\Delta\kappa$ and Δs) correspond to the mean acceptance rate closest to 30% (see Supplementary Sec. S1.1 for details). Here, the pair $\Delta\kappa$ and Δs are shown for an arbitrary pit SBP4 (Table 1 in the main text), and the selected pair are denoted by the open red circle.

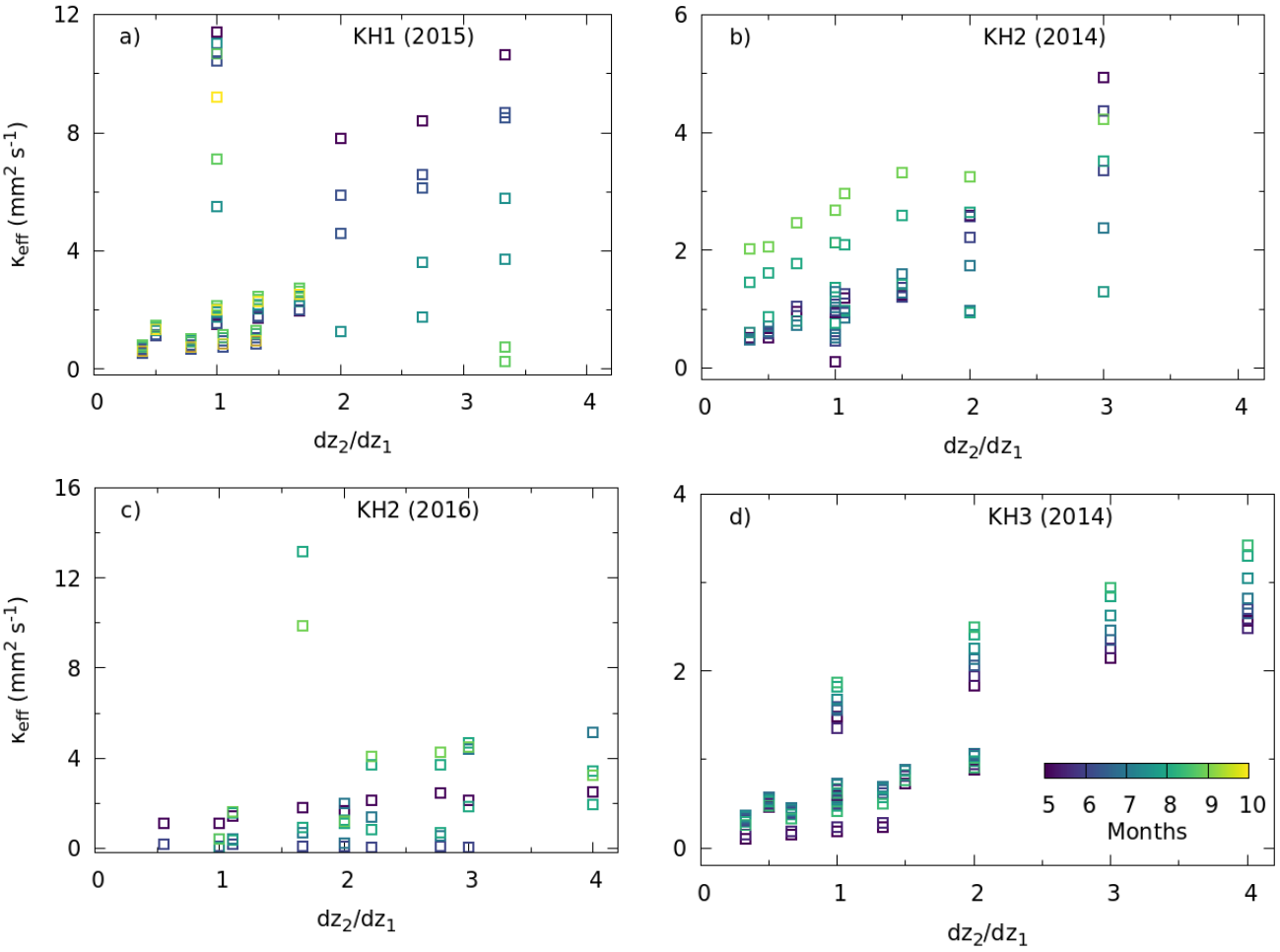

Fig. S5: The CR_h method estimates of κ_{eff} plotted for different dz_2/dz_1 from Khumbu Glacier during the ablation season of 2014–2016 for different pits (Rowan and others, 2021).

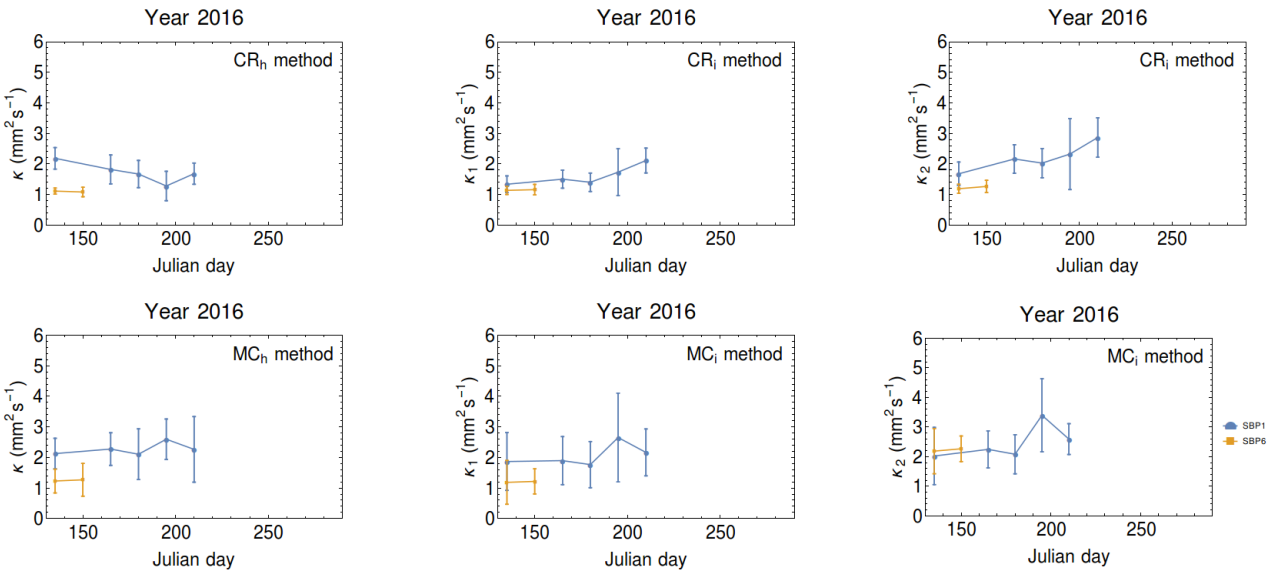

Fig. S6: The seasonality of estimated κ for all the four methods during the 2016 ablation season. Different colours and symbols denote different pits.

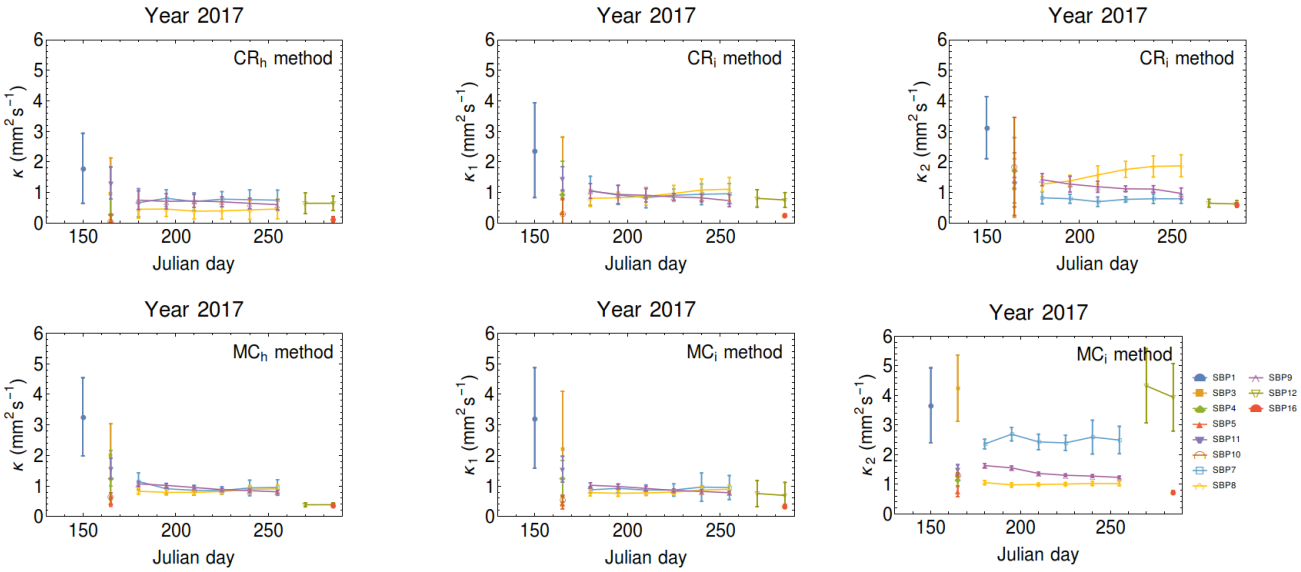

Fig. S7: The seasonality of estimated κ for all the four methods during the 2017 ablation season. Different colours and symbols denote different pits.

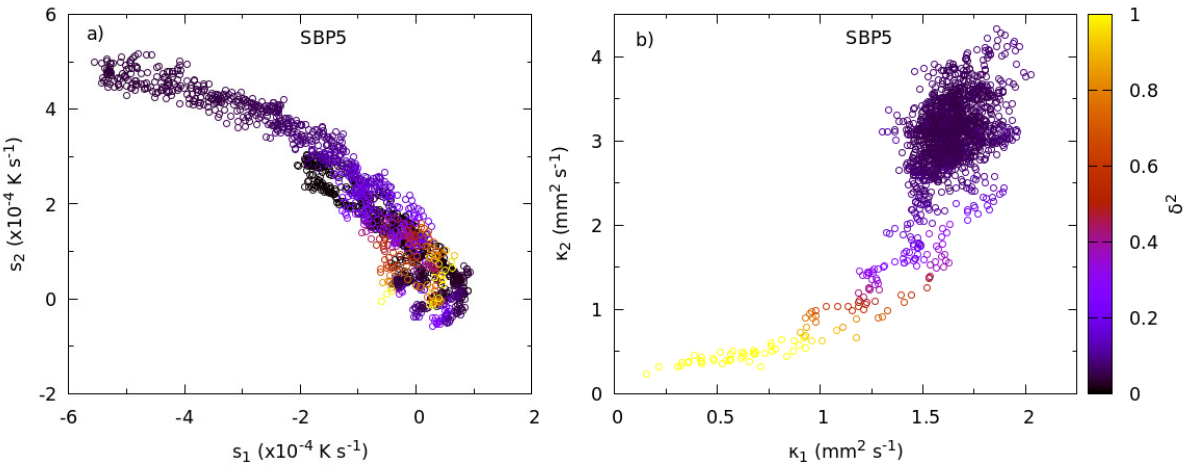

Fig. S8: For an arbitrarily chosen pit SBP5 (Table 1 in the main text), a) s_1-s_2, and b) κ_1-κ_2 values of all the accepted models from the last 5000 iterations of the MC_i method, where each point is coloured by the corresponding δ^2 of the fits. Here, the models are not covering the whole s_1-s_2 plane, rather these two parameters are anti-correlated with all points roughly on the s_1+$s_2 \sim 0$ line. Also, the corresponding δ^2 did not change significantly along this line compared to that of the κ_1-κ_2 plane.

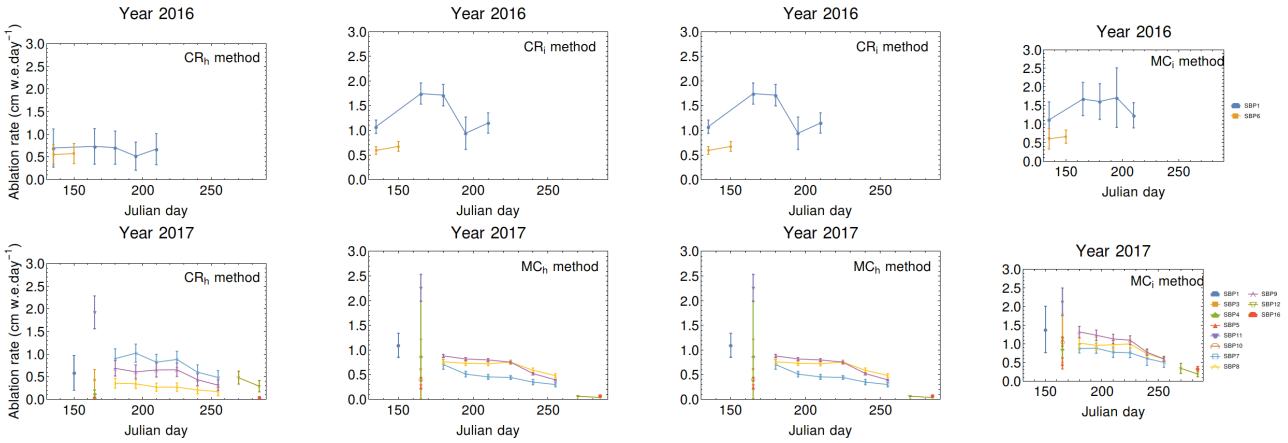

Fig. S9: Sub-seasonal ablation rates obtained from all the four methods with the corresponding estimated uncertainties for the ablation seasons 2016 and 2017. Different colours and symbols denote different pits.

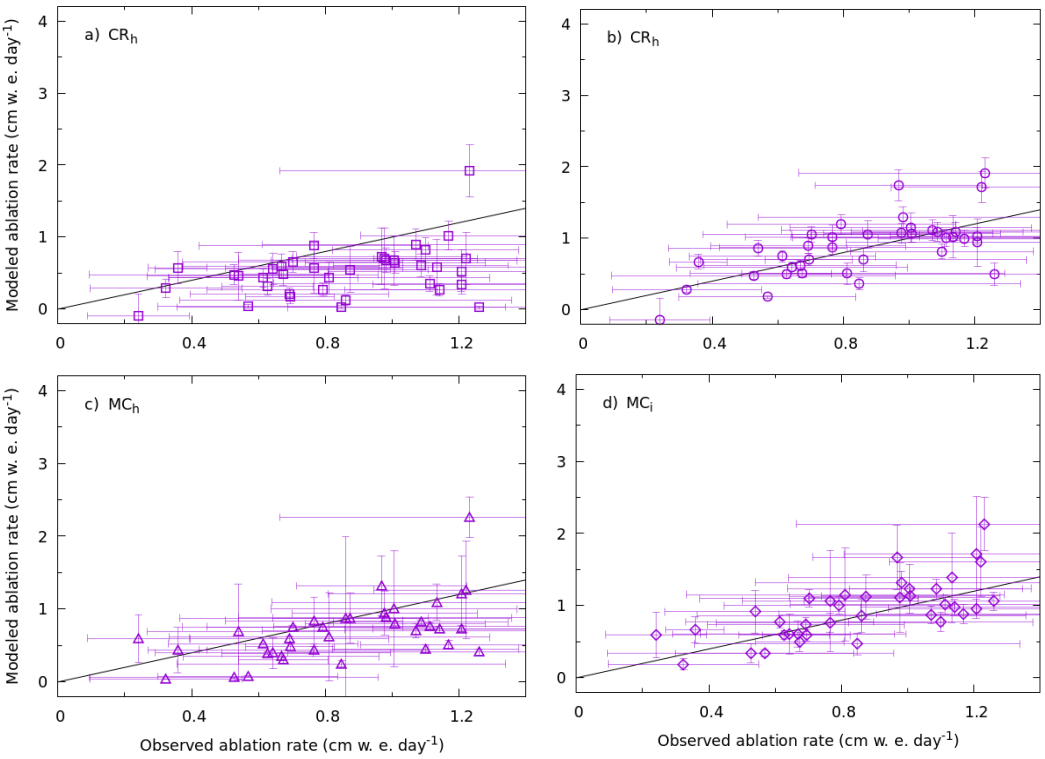

Fig. S10: Comparison of ablation rate estimates obtained from the (a) CR_h, (b) CR_i, (c) MC_h, (d) MC_i methods with that obtained from the observed glaciological method using ablation stakes. Here we plotted only the selected records (see Sec. 5.4 for more details) with the corresponding uncertainties. The solid grey line is a guide to the eye that denotes perfect match.